energies

MDPI

Review

Lithiated Manganese-Based Materials for Lithium-Ion Capacitor: A Review

Ntuthuko W. Hlongwa [1,*] and Naledi Raleie [2]

[1] Institute for Nanotechnology and Water Sustainability, College of Science, Engineering and Technology, Florida Campus, University of South Africa, Johannesburg 1710, South Africa
[2] Department of Chemistry, School of Mathematical & Physical Sciences, North-West University (Mafikeng Campus), Private Bag X2046, Mmabatho 2735, South Africa
* Correspondence: hlongnw@unisa.ac.za

Abstract: Lithium-ion capacitors (LICs) are a novel and promising form of energy storage device that combines the electrode materials of lithium-ion batteries with supercapacitors. They have the potential to deliver high energy density, power density, and long cycle life concurrently. Due to the good electrochemical performance of lithiated manganese-based materials in LICs, they have received extensive attention in recent years. The latest advancements in lithiated manganese-based materials as electrode materials in lithium-ion capacitors are presented here, including $LiMnPO_4$, $LiMn_2O_4$, and Li_2MnSiO_4. These electrode materials have a lot of potential as high-performance energy storage materials. Apart from capacitive-type electrodes, lithiated manganese-based materials are also used in the creation of LIC battery-type electrodes. The LICs based on lithiated manganese-based electrode materials demonstrated energy density, power density, and cycle life, which are relatively comparable with various electrode material values reviewed in this paper. The electrochemical performance of lithiated manganese-based materials is attributed to the synergistic effect of the doping and the conductive carbon coating which provided new pathways for the movement of Li^+ ions and electrons, thus facilitating charge transfer reactions. Although much effort has gone into synthesizing lithium-ion battery electrode materials and contracting LICs based on them because of their higher energy density, there is still work to be carried out. Additionally, the potential barriers and opportunities for LIC-based future research in energy applications are explored.

Keywords: lithium manganese oxide; lithium manganese phosphate; lithium manganese silicate; lithium-ion capacitors; energy density; power density

check for updates

Citation: Hlongwa, N.W.; Raleie, N. Lithiated Manganese-Based Materials for Lithium-Ion Capacitor: A Review. *Energies* **2022**, *15*, 7276. https://doi.org/10.3390/en15197276

Academic Editors: Mojtaba Mirzaeian, Peter Hall, Desmond Gibson, Saule Aidarova and Quanqing Yu

Received: 17 May 2022
Accepted: 27 September 2022
Published: 4 October 2022

1. Introduction

Electrochemical energy storage devices with high energy and power densities are essential for meeting the need and rapidly increasing global demand for sustainable energy supply. The performance of energy storage devices is primarily influenced by the active components and cell architecture. The main test in the development of energy storage devices is the balanced relationship between power and energy density. Energy storage systems such as lithium-ion capacitors are chosen based on two performance characteristics: the amount of energy they can store (energy density) and the speed with which they can be charged and discharged (power density). The Ragone plot is a plot used for comparing the energy and power densities of various energy storing devices, as shown in Figure 1. On such a chart, the values of specific energy (in W h kg^{-1}) are plotted versus specific power (in W kg^{-1}). The energy density of lithium-ion batteries (LIBs) is high (>10 W h kg^{-1}) with lower power density (1 kW kg^{-1}) and cycle life of about 300 to 500 charge cycles, while supercapacitors (SCs) have a high power density (>10 kW kg^{-1}) and lower energy density (5–10 W h kg^{-1}) [1–4]. Both lithium-ion batteries and supercapacitors have drawbacks that limit their use in some industries. Lithium-ion capacitors (LICs), or hybrid capacitors, were

designed to bridge the gap between LIBs and SCs. They incorporate the benefits of both LIBs and SCs. A LIC device usually consists of a high-capacity battery-type electrode and a high-rate capacitor-type electrode, both of which are connected by an electrolyte.

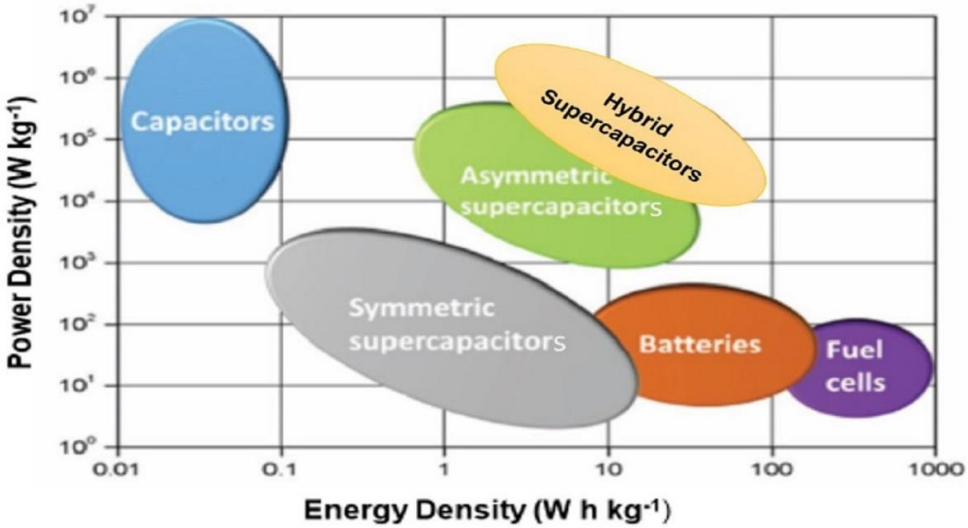

Figure 1. Ragone plot—comparison of the performance of different energy storage devices. Reproduced with permission [5]. Copyright 2017, Wiley-V.CH.

Hybrid capacitor devices are gaining popularity because of their higher energy and power density combined with good cycle stability. In hybrid capacitors, the capacitor-type electrode might be the anode or cathode, while the battery-type electrode is the counter electrode. It is worth mentioning that the capacitor-type and battery-type electrodes operate in separate potential windows, allowing hybrid capacitors to operate over a wider voltage range and achieve higher energy densities. Hybrid capacitors' energy and power densities are mostly determined by the electrode materials used in the devices. In recent years, much research has focused on developing the electrodes utilized in LICs. As a result, various kinds have been shown to perform differently in LIC architectures. A list of current studies on various materials is provided in Table 1.

Table 1. Summary of energy/power densities of LIC electrode.

Device Configuration (Anode//Cathode)	Voltage Range (V)	Cycling Stability	Maximum Energy Density (W h kg^{-1})	Maximum Power Density (W kg^{-1})	Ref.
N-doped carbon nanopipes//rGO	0–4	91% over 4000 cycles	262	9000	[6]
B&N-doped carbon nanofiber// B&N-doped nanofiber	0–4.3	81% over 5000 cycles	220	22,500	[7]
Graphite//graphene	2–4	97% over 3500 cycles	135	1500	[8]
Commercial graphite//activated carbon	2–4.5	69% over 2500 cycles	125	69	[9]
$Li_4Ti_5O_{12}$//graphite	1.5–3.7 V	88% over 10,000	233	20,960	[10]
Artificial graphene//$Na_{0.76}V_6O_{15}$	1–3.8 V	70% over 5000 cycles	119	21,793	[11]
TiO_2 nanobelt arrays//graphene hydrogels	0–3.8	73% over 600 cycles	82	19,000	[12]
Silicon/flake graphite/carbon nanocomposite//biomass-derived porous carbon	2–4.5 V	80% over 8000 cycles	159	31,235	[13]
$Li_4Ti_5O_{12}$-CNT//graphene foam	1–3.6	84% over 5000 cycles	101.8	12,300	[14]
MnO on C//trisodium citrate-derived carbon	0–3.9	85.69% over 10,000 cycles	235	25,000	[15]

Amatucci et al. were the first to develop hybrid capacitors in 2001 [16]. The research has grown in popularity since then. Although advancement in hybrid capacitor systems

has been addressed in various energy storage evaluations, there has not been a thorough review focused on lithiated manganese-based materials for lithium-ion capacitors. The essential idea of LICs will be described in this paper, as will the lithiated manganese-based battery-type electrode materials and their resurrection throughout several decades. The major roles of lithiated manganese materials as active materials in the applications of LICs are then highlighted. After a brief overview, the potential and limitations of LICs are reviewed, providing a detailed understanding of lithiated manganese-based electrodes for future LIC research.

2. The Bases of Electrochemical Capacitors

As seen in Figure 2, there are three main categories of supercapacitors: electric double-layer capacitors (EDLCs), pseudocapacitors, and asymmetric supercapacitors. Asymmetric supercapacitors can be divided into two categories: hybrid capacitors and systems with two capacitive electrodes. One electrode of hybrid capacitors is known to store charge via a battery-like Faradaic process, while the other electrode does it using a capacitive mechanism. The reversible adsorption of electrolyte ions on the surface of the active material stores energy in EDLCs, storing charge electrostatically rather than using a Faradaic (redox) process [17–19].

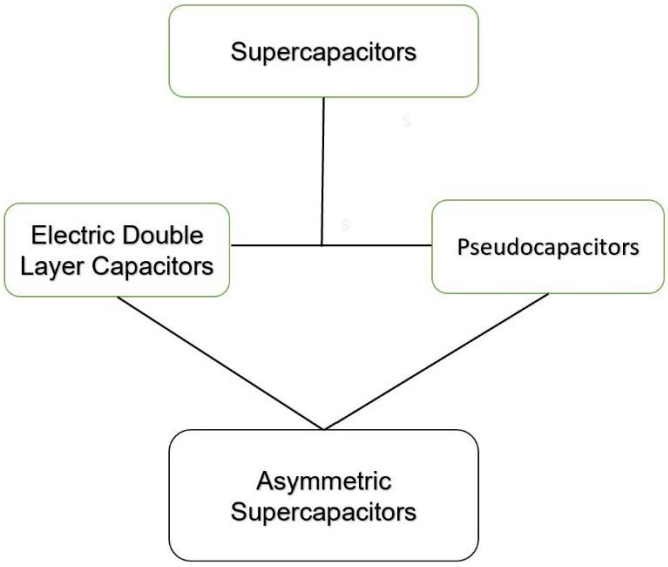

Figure 2. Schematic of types of supercapacitors.

To avoid electrical contact, EDLC cells typically have two carbon-based electrodes separated by a separator immersed in an electrolyte. Nanoporous materials with a large specific surface area (1000 m^2 g^{-1}) are active materials for EDLCs [20]. In 1879, Helmholtz defined the energy storage mechanism for EDLCs, and Stern and Geary improved it later.

Activated carbon (AC) is a widely accessible EDLC electrode with a cell voltage in an organic electrolyte of up to 2.7 V, a high power density (up to 10 kW kg^{-1}), and a long cycle life (1,000,000) [16,21]. The energy density, on the other hand, is still lower than 10 W h kg^{-1} [4,22–24]. The reduced energy density is owing to the AC electrode's low capacitance and high ionic resistance [25,26]. Therefore, this limits their application and they cannot meet the various performance demands required by the markets.

The charge storage process of pseudocapacitors (PCs) is based on reversible reactions between the electrolyte and electrode surface. PCs rely on quick redox reactions [25,27,28]. Transition metal oxides, conducting polymers, nitrides, carbines, and hydroxides are examples of common materials [29–31]. Electroanalytical investigations can separate PC electrode materials from battery electrode materials because their kinetics are constrained by a surface-related mechanism rather than diffusion-controlled processes that regulate the electrochemical response of battery electrodes [20]. The capacitance of PCs with transition

metal oxide (TMO) electrodes has been reported to be between 300 and 1000 F g^{-1} [28,32], however, due to very unpredictable cycling behavior over a few cycles, they suffer from capacity fading. The specific energy density of pseudocapacitors with an asymmetric configuration of two metal oxides is 5–10 W h kg^{1}. The behavior of the lithiated manganese-based electrodes (LMP, LMO, and LMSO) reviewed in this paper resembles that of PCs [33–36]. Since the energy density is a product of capacitance and voltage, increasing the voltage is necessary to enhance the energy density. Increasing the voltage is more effective because the energy density increases in proportion to squared voltage. Essentially, there have been three main approaches to achieving this goal: the first is to develop alternative carbonaceous or redox materials with higher capacitance; the second is to develop a novel electrochemically durable electrolyte or an ionic electrolyte with a large, stable voltage window; and the third and most promising approach under serious investigation is the development of non-aqueous Li-ion capacitors (LICs), also called hybrid Li-ion supercapacitors, which have the potential to essentially increase the voltage.

Lithium-ion capacitors (LICs) are hybrid capacitors made up of two electrode materials, one of which stores charge electrostatically and the other of which store's charge Faradaically. LICs are intended to bridge the gap between high-energy Li-ion batteries and high-power supercapacitors by combining their major benefits into a single device [31]. It is necessary to first define the components of LICs before comprehending their fundamental energy storage mechanism. A LIC is a hybrid supercapacitor that has a battery-type electrode for lithium-ion insertion/extraction and a capacitor-type electrode for pseudocapacitance or ion adsorption/desorption, while an asymmetric supercapacitor is assembled using two dissimilar electrode materials (pseudocapacitors and EDLCs) and offers a distinct advantage of a wide operational voltage window, thereby significantly enhancing the energy density.

3. Lithium-Ion Capacitor Materials

3.1. The Mechanism of the Lithium-Ion Capacitor

Lithium-ion capacitors combine the energy storage mechanisms of batteries and supercapacitor-type electrode materials in an electrolyte containing lithium ions. The charge storage mechanism in lithium-ion capacitors is the development of an EDL at the supercapacitor electrode and ion intercalation/de-intercalation at the Li-ion battery-type electrode [28,30,37]

The charge/discharge process, as depicted in Figure 3, involves the transfer of a lithium ion between two electrodes, with the electrolyte serving primarily as an ionic conductor. Amatucci et al. were the first to suggest or propose LIC principles when they created a 2.8 V hybrid capacitor using $Li_4Ti_5O_{12}$ (LTO) [38]. Due to its zero-strain qualities, Ohzuku et al. identified LTO to be an ideal Li intercalating spinel anode material for Li-ion battery applications. It has a high-rate capability and a specific capacity of 150 mA h g^{-1} [39]. The battery-type electrode can function as both an anode and a cathode, and the LICs are split into two types: (a) in an LTO/AC system, the anode is a battery-type electrode, while the cathode is a capacitor-type electrode, which was demonstrated by Amatucci and co-workers; (b) when the anode is the capacitor-type electrode, and the cathode is the battery-type electrode. Here, similar to a battery, charges are stored by a Faradaic reaction that occurs by solid-state diffusion of the ions into the electrode. This process leads to phase changes during the charging–discharging process which leads to less stability. These two mechanisms are shown in Figure 3.

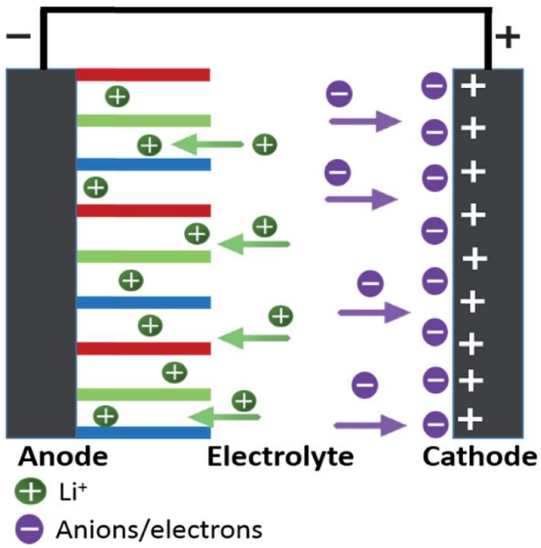

Figure 3. Mechanism of working lithium-ion capacitor.

As previously stated, the purpose of the battery type (Faradaic) electrode is to insert/de-insert Li-ions with a relatively constant voltage, resulting in a large specific capacity. The purpose of the non-Faradaic capacitor electrode is to adsorb and de-adsorb ions. These processes are reversible in varied ranges. The charge at each contact and the voltage difference between two plates determine the amount of energy stored in a capacitor (anode and cathode). The following equation is used to calculate the energy densities of the LIC.

$$\boldsymbol{E} = \int \boldsymbol{VdC} \tag{1}$$

The operating voltage is $\boldsymbol{V}$, and the capacitance is $\boldsymbol{C}$. Operating voltage has a direct relationship with both energy and power, and it plays a significant role in both. Optimizing the voltage window improves the electrochemical performance of LICs significantly. To enhance the quantity of energy that can be stored, a high operating voltage is required. To achieve this, three-electrode experiments for each electrode are required to (i) estimate the specific capacitance of materials, (ii) understand the electrolyte stability under a working environment, (iii) calculate contributions of surface and diffusion-controlled currents in hybrid systems, (iv) during charge/discharge operations, determine the oxidation and reduction potentials of active materials.

The mass ratio between the battery-type and the capacitor-type electrodes, as well as the intrinsic behavior of the battery-type and capacitor-type electrodes, has a significant impact on the cycle life of LICs. The charges at both electrodes should be balanced in an asymmetric cell ($q_{anode} = q_{cathode}$). The voltage must be shared evenly between the two electrodes using the mass balancing equation: $q_{cathode} = q_{anode}$, where $q_{cathode}$ represents the charges stored at the positive electrode and q_{anode} represents the charges stored at the negative electrode. The formulae for the charge stored are as follows:

$$q = Csp \cdot m \cdot \Delta E \tag{2}$$

or

$$\frac{m_{cathode}}{m_{anode}} = \frac{Csp_{anode} \times \Delta E_{anode}}{Csp_{cathode} \times \Delta E_{cathode}}, \tag{3}$$

where m represents mass, ΔE denotes the potential window calculated from the charge/discharge patterns of the three-electrode arrangements of the negative and positive electrodes, respectively, and Csp refers to specific capacitance. The electrode material determines the capacitance and stored energy to a large extent. Specific capacitance (Csp) and equivalent series resistance, which are influenced by pore size distribution, specific surface

area, and electrode material conductivity, are two more key components in increasing LIC performance [25,40,41].

The discrepancy in power capability and charge storage capacitance between the two electrodes used in producing high-performance LICs is one of the problems in developing them. Limiting cycling-induced electrode degradation, particularly at high rates, to match the high-power properties of anode carbon-based materials is the most difficult component of constructing a Li intercalation cathode. Due to its lower capacity (30–35 mA h g^{-1}) compared to cathodes, the carbon-based anode has difficulties, further diminishing the energy density [42]. This paper summarizes the electrochemical activity of lithiated manganese-based materials and their relevance in LIC applications. Furthermore, the review evaluates the material modifications for fast ions and electron transport, such as thin-film design, porosity enhancement, nanostructuring, and composite design.

3.2. Design and Development of Lithiated Manganese-Based Materials for Li-Ion Capacitors

Lithium-ion batteries offer the highest energy and power densities of all commercially available batteries. As a result, lithium-ion chemistries may be used in hybrid supercapacitors to attain useful energy and power characteristics. Lithium-ion technologies in non-aqueous fluids have progressed considerably in the consumer electronics and grid energy storage industries [43–45]. Lithium-ion technologies have now surpassed all others in consumer electronics and electromobility when it comes to maximum energy density. However, in grid energy storage applications where cost is more essential than energy density, cost-effective analog technologies could be considered. The abundance rank and cost (USD kg^{-1}) of lithium, as well as sodium, potassium, magnesium, zinc, calcium, and aluminum, are shown in Figure 4 [46].

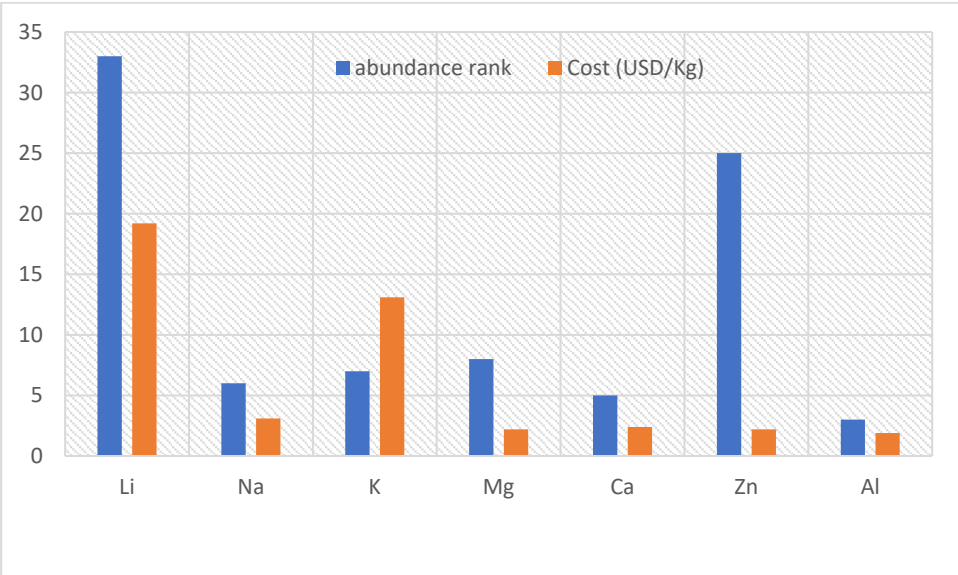

Figure 4. Different charge carriers' relative abundance rank and cost (Li^+, Na^+, Mg^{2+}, Ca^{2+}, Zn^{2+}, and Al^{3+}) for rechargeable batteries.

Employing lithiated manganese-based electrode materials in lithium-ion capacitors is advantageous due to the high energy density, design flexibility, and long cycling capabilities of lithium-ion chemistries [47–49]. Manganese or its oxides are appealing for hybrid supercapacitors because it is a transition metal with five unpaired electrons and the most oxidation states in the periodic table, including the highest oxidation state (VII). Manganese's unique electronic structure makes it redox-active and it exists in a variety of oxide forms (including MnO, MnO_2, Mn_2O_3, Mn_3O_4 ($MnO{\cdot}Mn_2O_3$), and Mn_2O_7) [49,50]. Second, among pseudocapacitive oxides, manganese is the most common transition metal. This review discusses progress in the development of better LICs using lithiated manganese-based

electrodes (lithium manganese oxide ($LiMn_2O_4$), lithium manganese phosphate ($LiMnPO_4$), lithium manganese silicate (Li_2MnSiO_4)), as well as nanocomposite. A few figures from the selected publications are briefly shown for better understanding.

3.2.1. Lithium Manganese Phosphate

The lithium manganese phosphate ($LiMnPO_4$) cathode has received a lot of interest because of its high operating voltage (4.1 V vs. Li) and ability to produce a maximum energy density of 700 W h kg^{-1}, outperforming the commercially available cathodes of lithium cobalt oxide (518 W h kg^{-1}), lithium manganese oxide (400 W h kg^{-1}), and lithium iron phosphate (495 W h kg^{-1}) [51–53]. Olivine compounds have been extensively studied as positive electrodes in lithium-ion batteries and they have demonstrated several advantages, including being economically valuable, environmentally friendly, and having excellent thermal stability [54–56]. In a $LiMnPO_4$ olivine structure, the O atoms are arranged in a hexagonal close-packed configuration, while the MnO^6 octahedron is separated by the PO_4 polyanion. Mn and Li occupy the octahedral 4c and 4a positions, respectively, with the P atom in the 4c site [51]. All oxygen ions in $LiMnPO_4$ form strong covalent bonds with P^{5+} in the tetrahedron to form PO_4^{3-} polyanion which stabilizes the entire three-dimensional framework as shown in Figure 5 [57–59]. Due to their increased stability, olivine cathode materials have the benefit of being able to function in harsh environments while being safe. $LiMnPO_4$ has a higher working voltage of 4.1 V, which is within the non-aqueous electrolyte's stability window, and a theoretical capacity of 170 mA h g^{-1} [46–48].

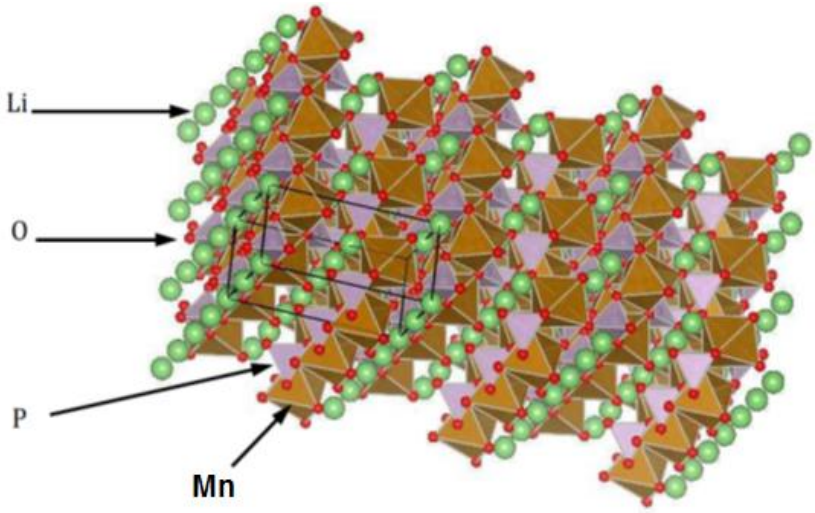

Figure 5. Structure of the $LiMnPO_4$ [60].

3.2.2. Lithium Manganese Oxide

One of the most promising lithium-ion battery cathodes is lithium manganese oxide ($LiMn_2O_4$) with a spinel structure. They are low-cost, safe, and produce 400 W h kg^{-1} of theoretical energy. The lattice spinel $LiMn_2O_4$ contains cubic close-packed oxygen ions while the cations are distributed among the available octahedral and tetrahedral sites, providing structural stability [61–64]. Mn cations occupy half of the octahedral interstitial sites and one-eighth of the tetrahedral sites. The interstitial space in the $[Mn_2]O_4$ framework, as illustrated in Figure 6, consists of a diamond-like network of tetrahedral surrounding octahedral sites that share edges and faces to create 3D diffusion routes for Li^+ ions diffusion [64–66]. The discharge occurs in two phases, one at 4 V and the other at 3 V with a capacity of $\leq$120 mA h g^{-1} [53,67–70]. Only the 4 V plateau is typically used, implying that the cell is built in a depleted condition and must be charged before use. The structure's cubic symmetry does not change throughout cycling, and the unit cell compresses very slightly across a wide range of compositions, confirming the structure's stability.

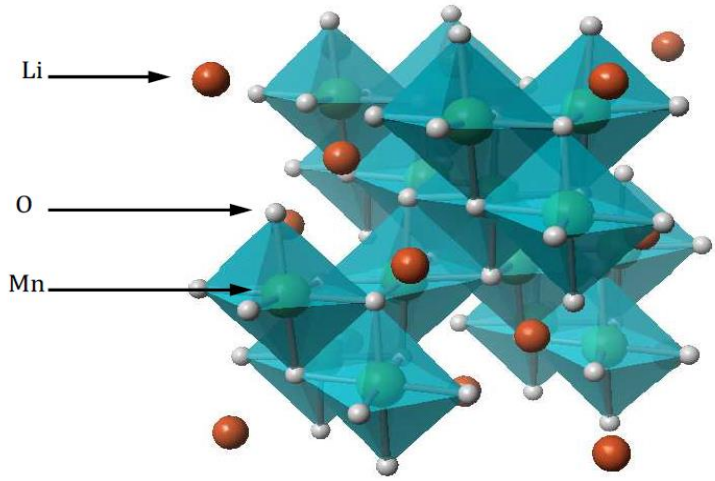

Figure 6. Structure of spinel $LiMn_2O_4$. Reproduced with permission [71]. Copyright 2013, Elsevier.

3.2.3. Lithium Manganese Silicate

Lithium orthosilicates, Li_2MSiO_4 (M = Mn, Fe, Co), have caught the attention of several researchers as high-capacity electrode materials for Li-ion batteries and hybrid supercapacitors [61–63]. Due to their many enticing qualities, including their high theoretical capacity (330 mA h g^{-1}) when more than one lithium ion is extracted per formula unit, they are becoming increasingly popular [72–74]. The extraction of more than one lithium ion per formula unit provides high thermal stability [35]; Li_2MnSiO_4 is a more promising orthosilicate electrode material because it allows for the reversible extraction of two moles of Li^+ ions utilizing the Mn^{2+}/Mn^{3+} and Mn^{3+}/Mn^{4+} redox couples, and this results in a greater energy density [74,75]. Li_2MnSiO_4 has an orthogonal structure. The orthorhombic forms (P*mn*2_1 and P*mnb*) have two-dimensional channels for Li-ion diffusion, whereas the monoclinic forms (P2_1*ln* and P*n*) have three-dimensional routes (see Figure 7). The 2D structures are destabilized when Li-ion is eliminated.

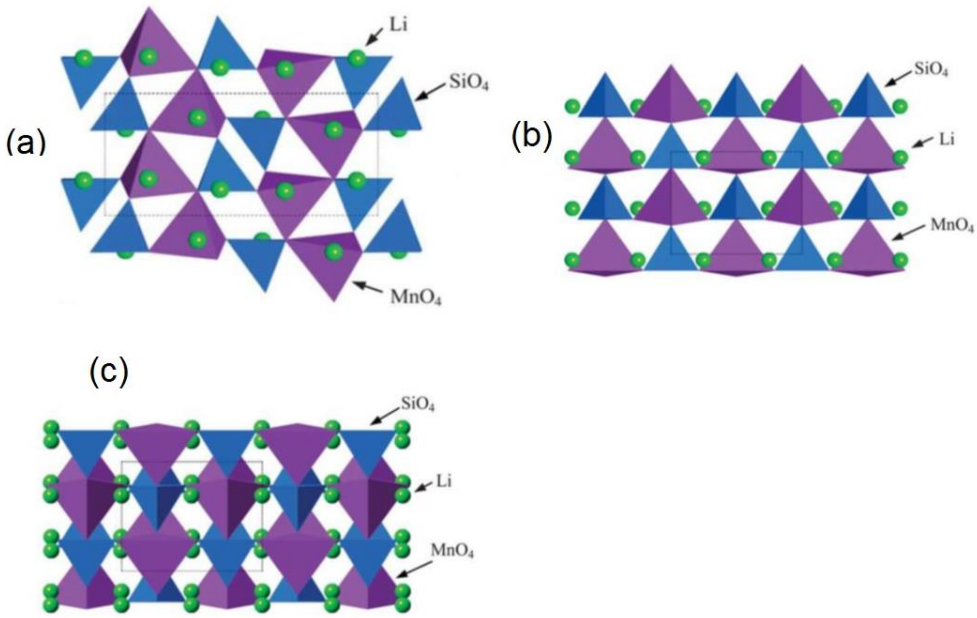

Figure 7. Crystal structures of Li_2MnSiO_4 polymorphs: (**a**) monoclinic P21/n phase, (**b**) orthorhombic Pmn21 phase orthorhombic Pmnb phase, (**c**) orthorhombic Pmnb phase, revealing the arrangement of MnO_4 tetrahedra (purple), SiO_4 tetrahedra (blue) with Li-ions (green). Reproduced from [76] with permission from the Royal Society of Chemistry.

4. Application of Lithiated Manganese-Based Materials as Lithium-Ion Capacitors

Several investigations on lithiated manganese-based electrodes have been undertaken to determine their use in LICs. Other lithium-based positive electrodes were used in Wang and co-workers' studies [77]. Several studies on lithium-ion capacitors have yielded promising results, with lithium metal phosphates, spinel oxides, and manganese silicate having been investigated as the promising electrode material.

Yang et al. created a $LiMn_2O_4$//nitrogen-doped graphene/porous carbon composite in an aqueous 0.5 M Li_2SO_4 with a specific energy of up to 44.3 W h kg^{-1}, a specific power of 595 W kg^{-1}, and an output voltage of 1.8 V [78]. Using an aqueous $LiNO_3$ electrolyte, Yen-Po Lin and Nae-Lih Wu produced $LiMn_2O_4$//$MnFe_2O_4$ cells with a specific energy of 5.5 W h kg^{-1} and a power density of 1.8 kW kg^{-1} under a maximum working voltage window of 1.3 V [79]. Pazhamalai and colleagues used an aqueous 1 M Li_2SO_4 electrolyte with an operating voltage of 2.2 V to create an asymmetric $LiMn_2O_4$//graphene LIC with high specific energy of 30.96 W h kg^{-1} and a power density of 440 W kg^{-1} [80]. Liu and co-workers assembled a $LiMn_2O_4$//WO_3 all-inorganic electrochromic Li-ion hybrid supercapacitor which demonstrated a volumetric energy/power density of 16.2 W cm^{-3}/0.21 W h cm^{-3} at a working voltage of 2.5 V and remarkable cycling stability with 95.4% capacitance retention after 5000 cycles [81]. However, high ionic and electrical resistance hinder further improvements for lithiated manganese-based materials in their electrochemical activity. In addition, Table 2 contains several other potential LICs.

Table 2. Lithiated manganese-based material LIC summary.

Device Configuration (Anode//Cathode)	Voltage Rage (V)	Cycling Stability	Maximum Energy Density (W h kg^{-1})	Maximum Power Density (W kg^{-1})	Ref.
AC//$LiMnPO_4$	0–2	83% over 1000 cycles	28.8	2500	[82]
$LiMn_2O_4$//nitrogen doped graphene	0–1.8	85 % over 1000 cycles	44.3	595	[78]
$LiMn_2O_4$//graphene	0–2.2	90% over 1000 cycles	39.96	440	[80]
$LiMn_2O_4$//AC	0–2	75.9% over 2000 cycles	32.63	10,000	[83]
Li_2MnSiO_4//AC	0–1.3	95% over 5000 cycles	7.75	1650	[84]
Porous nanosized Li_2MnSiO_4	0–0.6	90% over 500 cycles	7	135	[85]

4.1. Effect of Doping on the Pristine Material

Doping is the process of introducing small amounts of a semiconductor element to a material to change or regulate its electrical characteristics. Extrinsic semiconductors are those that have been lightly doped, whereas degenerates are those that have been doped to such great degrees that they behave more like a conductor than a semiconductor [86]. Doping refers to the process of activating a substance. Despite their potential, manganese-based electrode materials suffer from considerable capacity loss during cycling [87–90]. The presence of Jahn–Teller distortion, which is caused by Mn^{3+} and results in lower cyclability during the Li^+ diffusion process, is the main reason for this.

Doping manganese cathode materials can reduce manganese dissolution and Jan–Teller distortion and raise power and energy density while improving conductivity and maintaining and improving the capacity of active materials [91]. Several studies have used various doping techniques to modify the surface of manganese-based cathode materials. However, the search for new electrode materials with lower costs and better properties is still important in the development of lithium-ion capacitors. Table 3 further highlights the energy and power densities of recently developed LIC-based manganese-based doped materials.

Table 3. Summary of energy/power densities of LICs on basis of doped manganese-based material.

Device Configuration (Anode//Cathode)	Voltage Range (V)	Cycling Stability	Maximum Energy Density (W h kg^{-1})	Maximum Power Density (W kg^{-1})	Ref.
AC//$LiMn_{0.95}Ni_{0.05}PO_4$	0–2	71% over 800 cycles	9.4	1610	[34]
$LiNd_{0.01}Mn_{1.99}O_4$//black pearl carbon	0–1.6	86 % over 2500 cycles	17	397	[66]
AC//Li_2MnSiO_4/Al_2O_3	0–2.2	93.6% over 100 cycles	10.4	4020.8	[35]
$LiMn_2O_4$@$LiNbO_3$//WO_3	0–2.3	83.5% over 3000 cycles	106.1	574.7	[92]

4.2. Effect of Carbon on the Pristine Material

The electrochemical performance of manganese-based materials, for example, may be improved by the surface coating, in lithiated manganese-based materials lowering Mn^{2+} and enhancing lithium-ion transit [7,93]. For high-rate manganese-based cathode materials, carbon coating is required, and the quality of the carbon coating has a significant influence on the lithium-ion cathode material. Different research groups looked at manganese-based materials created with various carbon sources to see if carbon coating increases conductivity and rate performance.

Due to their remarkable properties, carbon-based materials have been employed in a variety of research sectors, particularly in the field of energy storage, due to their outstanding qualities. Graphene, for example, is a one-atom-thick sheet of sp^2-connected carbon atoms with a polyaromatic honeycomb crystal structure [20]. With a large specific surface area of 1500 m^2 g^{-1}, high electrical conductivity of 106 S cm^{-1}, good flexibility and tuneability, good chemical and thermal stability, and a wide potential window, its thin monolayer structure delivers a good platform for the growth of great capacitive hybrid energy storage devices [27,31,32]. Figure 8 depicts a schematic representation of the $LiMnPO_4$/reduced graphene oxide aerogel produced by solvothermal treatment and subsequent restacking.

Figure 8. A schematic depiction of the $LiMnPO_4$/rGO aerogel preparation method. Reproduced with permission from [80]. Copyright 2018, Elsevier.

Carbon-based lithium-ion capacitors have been found to function better, with higher energy and power density, as well as faster charging and discharging over many cycles. Zhang et al. [94] developed an Fe_3O_4-graphene nanocomposite for LICs with a specific energy of 60.5 Wh kg^{-1} and a power density of 45.4 kW kg^{-1} in the 1–4 V potential window. At a voltage of 1–2.5 V, Lu and colleagues created a $Li_4Ti_5O_{12}$/graphene nanosheet composite for LICs that possessed specific energy of 14 W h kg^{-1} and a power density of 2.7 kW kg^{-1} [95]. Figure 9a–j display the performance testing results of LICs based on Li_2MnSiO_4/CNTs. The authors employed cyclic voltammetry, impedance spectroscopy, and galvanostatic charge/discharge to demonstrate the device's good performance in pow-

ering LED lights. Table 4 summarizes the performance of carbon-based coated manganese-based materials.

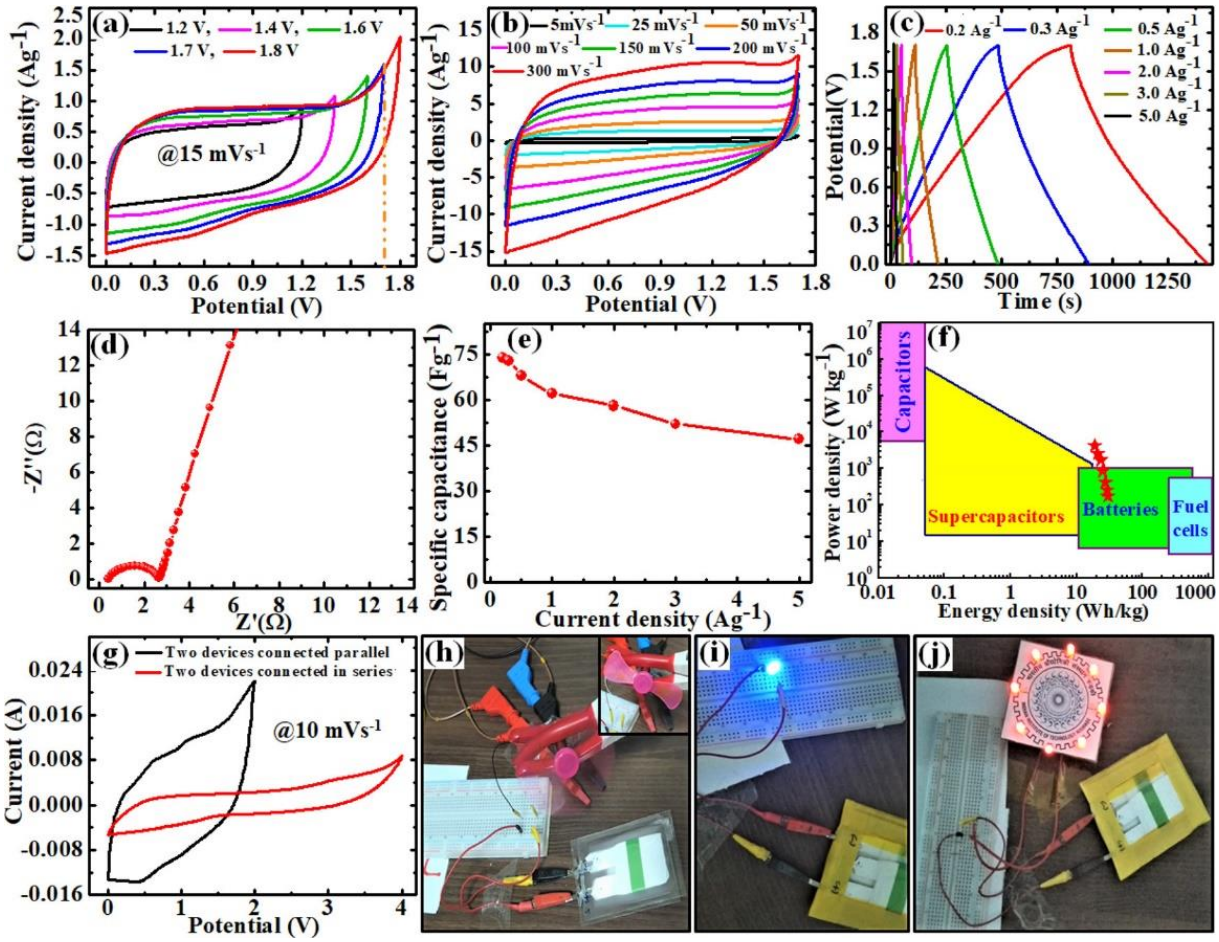

Figure 9. Lithium-ion capacitor performance of Li_2MNSiO_4/CNTs, (**a**) CV plots of nanocomposite @15 mV s^{-1}, (**b**) CV curve cell at different scan rates, (**c**) GCD curves at various current density values, (**d**) Nyquist plot of the device, (**e**) specific capacitance as a function of current density, (**f**) Ragone plot showing power density as a function of energy density for an asymmetric cell, (**g**) CV curves of two supercapacitor devices @ 10 mV s^{-1} when connected in series and parallel, (**h**) two parallel-connected devices powering a DC motor fan with inset showing the non-rotating motor fan, (**i**) two series-connected cells lighting up a blue LED, and (**j**) 8 red LEDs. Reproduced with permission [75]. Copyright 2020, American Chemical Society.

Table 4. Summary of the performance of carbon-based coated manganese-based materials.

Device Configuration (Anode//Cathode)	Voltage Range (V)	Cycling Stability	Maximum Energy Density (W h kg^{-1})	Maximum Power Density (W kg^{-1})	Ref.
AC//LMNP/graphene	0–2	83% over 750 cycles	14	1900	[34]
$LiMnPO_4$/rGO//rGO	0–1.5	91.2% over 10,000	16.46	4520	[96]
$LiMn_2O_4$/graphene//AC	0–2.3	90.6% over 500 cycles	38.8	12.6	[36]
$LiMn_2O_4$/graphene/CNs//N/S co-doped AC	0–2.1	90.8% over 5000 cycles	62.77	2967.96	[97]
Li_2MnSiO_4/CNTs//AC	0–1.6	83% over 2500 cycles	31	177	[74]

5. Conclusions and Perspectives

Increasing global demand for sustainable energy supply requires more efficient energy storage devices with high energy and power densities. The performance of energy storage devices depends mainly on the active materials and the design of the cell. Nowadays, the

development of novel materials is helping in the improvement of the required characteristics of energy storage devices. Therefore, it is an important technological task related directly to the commercial applications of these devices. Recently developed LICs are making their way into different commercial applications. LIC electrode materials have yet to reach their full potential. In comparison to other energy storage devices such as lithium-ion batteries, supercapacitors, etc., LICs are the only energy storage technology that provides high energy, power density, and longer cycle life. Optimizing interfacial interactions and the manufacture of uniform structures to improve charge transfer in high-performance energy storage systems using LICs requires a thorough understanding of the surface chemistry of capacitors and battery components. The present state of lithiated manganese-based materials as electrode materials in lithium-ion capacitors is summarized in this paper. The materials of choice were $LiMnPO_4$, $LiMn_2O_4$, and Li_2MnSiO_4. The energy density, power density, and cycle life values of the LICs based on lithiated manganese-based electrode materials were proven to be generally equivalent to those of various electrode materials. The electrochemical performance of lithiated manganese-based materials is attributed to the synergistic effect of the doping and the conductive carbon coating which provided new pathways for the movement of Li+ ions and electrons, thus facilitating charge transfer reactions. However, there is still more work to be carried out. For practical applications, electrodes with high power and energy, as well as better electrochemical and mechanical properties, should be investigated further. In the field of LICs, manganese-based materials will continue to push scientific and technical progress. LICs have achieved great progress in the last several years. Nonetheless, there are still many challenges to be tackled, both at fundamental levels as well as at practical application levels, to enable high-performance LICs in terms of materials and their properties.

Author Contributions: The manuscript was written and conceptualized by N.W.H. while N.R. conceptualized, reviewed, and edited the manuscript. All authors have read and agreed to the published version of the manuscript.

Funding: This research received no external funding.

Data Availability Statement: Not applicable.

Acknowledgments: Ntuthuko W. Hlongwa and Naledi Raleie acknowledge the support from the Institute for Nanotechnology and Water Sustainability at the University of South Africa and department of chemistry at the North-West University (Mafikeng Campus).

Conflicts of Interest: The authors declare no conflict of interest.

References

1. Du, H.; Yang, H.; Huang, C.; He, J.; Liu, H.; Li, Y. Graphdiyne applied for lithium-ion capacitors displaying high power and energy densities. *Nano Energy* **2016**, *22*, 615–622. [CrossRef]
2. Zhang, S.S. Dual-Carbon Lithium-Ion Capacitors: Principle, Materials, and Technologies. *Batter Supercaps* **2020**, *3*, 1137–1146. [CrossRef]
3. Lamb, J.J.; Burheim, O.S. Lithium-Ion Capacitors: A Review of Design and Active Materials. *Energies* **2021**, *14*, 979. [CrossRef]
4. Jin, L.; Yuan, J.; Shellikeri, A.; Naderi, R.; Qin, N.; Lu, Y.; Fan, R.; Wu, Q.; Zheng, J.; Zhang, C.; et al. An Overview on Design Parameters of Practical Lithium-Ion Capacitors. *Batter. Supercaps* **2021**, *4*, 749–757. [CrossRef]
5. Choudhary, N.; Li, C.; Moore, J.; Nagaiah, N.; Zhai, L.; Jung, Y.; Thomas, J. Asymmetric Supercapacitor Electrodes and Devices. *Adv. Mater.* **2017**, *29*, 1605336. [CrossRef]
6. Dubal, D.P.; Gomez-Romero, P. All nanocarbon Li-Ion capacitor with high energy and high power density. *Mater. Today Energy* **2018**, *8*, 109–117. [CrossRef]
7. Xia, Q.; Yang, H.; Wang, M.; Yang, M.; Guo, Q.; Wan, L.; Xia, H.; Yu, Y. High Energy and High Power Lithium-Ion Capacitors Based on Boron and Nitrogen Dual-Doped 3D Carbon Nanofibers as Both Cathode and Anode. *Adv. Energy Mater.* **2017**, *7*, 1701336. [CrossRef]
8. Lee, J.H.; Shin, W.H.; Lim, S.Y.; Kim, B.G.; Choi, J.W. Modified graphite and graphene electrodes for high-performance lithium ion hybrid capacitors. *Mater. Renew. Sustain. Energy* **2014**, *3*, 22. [CrossRef]
9. Nanaji, K.; Pappu, S.; Anandan, S.; Rao, T.N. A High-Energy Density Li-Ion Hybrid Capacitor Fabricated from Bio-Waste Derived Carbon Nanosheets Cathode and Graphite Anode. *Glob. Chall.* **2022**, 2200082. [CrossRef]

10. Wang, G.; Oswald, S.; Löffler, M.; Müllen, K.; Feng, X. Beyond Activated Carbon: Graphite-Cathode-Derived Li-Ion Pseudocapacitors with High Energy and High Power Densities. *Adv. Mater.* **2019**, *31*, e1807712. [CrossRef]
11. Lu, R.; Ren, X.; Wang, C.; Zhan, C.; Nan, D.; Lv, R.; Shen, W.; Kang, F.; Huang, Z.-H. $Na_{0.76}V_6O_{15}$/Activated Carbon Hybrid Cathode for High-Performance Lithium-Ion Capacitors. *Materials* **2021**, *14*, 122. [CrossRef] [PubMed]
12. Wang, H.; Guan, C.; Wang, X.; Fan, H.J. A High Energy and Power Li-Ion Capacitor Based on a TiO_2 Nanobelt Array Anode and a Graphene Hydrogel Cathode. *Small* **2015**, *11*, 1470–1477. [CrossRef] [PubMed]
13. Lu, Q.; Lu, B.; Chen, M.; Wang, X.; Xing, T.; Liu, M.; Wang, X. Porous activated carbon derived from Chinese-chive for high energy hybrid lithium-ion capacitor. *J. Power Sources* **2018**, *398*, 128–136. [CrossRef]
14. Liu, Y.; Wang, W.; Chen, J.; Li, X.; Cheng, Q.; Wang, G. Fabrication of porous lithium titanate self-supporting anode for high performance lithium-ion capacitor. *J. Energy Chem.* **2020**, *50*, 344–350. [CrossRef]
15. Zhang, J.; Lin, J.; Zeng, Y.; Zhang, Y.; Guo, H. Morphological and Structural Evolution of MnO@C Anode and Its Application in Lithium-Ion Capacitors. *ACS Appl. Energy Mater.* **2019**, *2*, 8345–8358. [CrossRef]
16. Amatucci, G.G.; Badway, F.; Du Pasquier, A.; Zheng, T. An Asymmetric Hybrid Nonaqueous Energy Storage Cell. *J. Electrochem. Soc.* **2001**, *148*, A930. [CrossRef]
17. Horn, M.; MacLeod, J.; Liu, M.; Webb, J.; Motta, N. Supercapacitors: A new source of power for electric cars? *Econ. Anal. Policy* **2019**, *61*, 93–103. [CrossRef]
18. Berrueta, A.; Ursua, A.; Martin, I.S.; Eftekhari, A.; Sanchis, P. Supercapacitors: Electrical Characteristics, Modeling, Applications, and Future Trends. *IEEE Access* **2019**, *7*, 50869–50896. [CrossRef]
19. Burke, A.F.; Zhao, J. Past, present and future of electrochemical capacitors: Technologies, performance and applications. *J. Energy Storage* **2021**, *35*, 102310. [CrossRef]
20. González, A.; Goikolea, E.; Barrena, J.A.; Mysyk, R. Review on supercapacitors: Technologies and materials. *Renew. Sustain. Energy Rev.* **2016**, *58*, 1189–1206. [CrossRef]
21. Faraji, S.; Ani, F.N. The development supercapacitor from activated carbon by electroless plating—A review. *Renew. Sustain. Energy Rev.* **2015**, *42*, 823–834. [CrossRef]
22. Xiao, X.; Han, B.; Chen, G.; Wang, L.; Wang, Y. Preparation and electrochemical performances of carbon sphere@ZnO core-shell nanocomposites for supercapacitor applications. *Sci. Rep.* **2017**, *7*, 40167. [CrossRef] [PubMed]
23. Wang, K.; Gao, S.; Du, Z.; Yuan, A.; Lu, W.; Chen, L. MnO_2-Carbon nanotube composite for high-areal-density supercapacitors with high rate performance. *J. Power Sources* **2016**, *305*, 30–36. [CrossRef]
24. Chen, C.; Yu, D.; Zhao, G.; Sun, L.; Sun, Y.; Leng, K.; Yu, M.; Sun, Y. Hierarchical porous graphitic carbon for high-performance supercapacitors at high temperature. *RSC Adv.* **2017**, *7*, 34488–34496. [CrossRef]
25. Wang, X.; Shi, B.; Fang, Y.; Rong, F.; Huang, F.; Que, R.; Shao, M. High capacitance and rate capability of a Ni_3S_2@CdS core–shell nanostructure supercapacitor. *J. Mater. Chem. A* **2017**, *5*, 7165–7172. [CrossRef]
26. Makgopa, K.; Ejikeme, P.M.; Jafta, C.J.; Raju, K.; Zeiger, M.; Presser, V.; Ozoemena, K.I. A high-rate aqueous symmetric pseudocapacitor based on highly graphitized onion-like carbon/birnessite-type manganese oxide nanohybrids. *J. Mater. Chem. A* **2014**, *3*, 3480–3490. [CrossRef]
27. Sui, D.; Chang, M.; Peng, Z.; Li, C.; He, X.; Yang, Y.; Liu, Y.; Lu, Y. Graphene-Based Cathode Materials for Lithium-Ion Capacitors: A Review. *Nanomaterials* **2021**, *11*, 2771. [CrossRef]
28. Suktha, P.; Phattharasupakun, N.; Dittanet, P.; Sawangphruk, M. Charge storage mechanisms of electrospun Mn_3O_4 nanofibres for high-performance supercapacitors. *RSC Adv.* **2017**, *7*, 9958–9963. [CrossRef]
29. Xu, N.; Sun, X.; Zhang, X.; Wang, K.; Ma, Y. A two-step method for preparing $Li_4Ti_5O_{12}$–graphene as an anode material for lithium-ion hybrid capacitors. *RSC Adv.* **2015**, *5*, 94361–94368. [CrossRef]
30. Kim, M.; Kim, J. Development of high power and energy density microsphere silicon carbide-MnO_2 nanoneedles and thermally oxidized activated carbon asymmetric electrochemical supercapacitors. *Phys. Chem. Chem. Phys.* **2014**, *16*, 11323–11336. [CrossRef]
31. Lu, X.; Yu, M.; Wang, G.; Tong, Y.; Li, Y. Flexible solid-state supercapacitors: Design, fabrication and applications. *Energy Environ. Sci.* **2014**, *7*, 2160–2181. [CrossRef]
32. Ma, Y.; Chang, H.; Zhang, M.; Chen, Y. Graphene-Based Materials for Lithium-Ion Hybrid Supercapacitors. *Adv. Mater.* **2015**, *27*, 5296–5308. [CrossRef] [PubMed]
33. Ko, J.S.; Sassin, M.B.; Rolison, D.R.; Long, J.W. Deconvolving double-layer, pseudocapacitance, and battery-like charge-storage mechanisms in nanoscale $LiMn_2O_4$ at 3D carbon architectures. *Electrochim. Acta* **2018**, *275*, 225–235. [CrossRef]
34. Hlongwa, N.W.; Ikpo, C.O.; Ndipingwi, M.M.; Nolly, C.; Raleie, N.; Dywili, N.; Iwuoha, E.I. Graphene-functionalised Olivine Lithium Manganese Phosphate Derivatives for High Performance Lithium-ion Capacitors. *Electroanalysis* **2020**, *32*, 2812–2826. [CrossRef]
35. Ndipingwi, M.M.; Ikpo, C.O.; Hlongwa, N.W.; Myalo, Z.; Ross, N.; Masikini, M.; John, S.V.; Baker, P.G.; Roos, W.D.; Iwuoha, E.I. Orthorhombic Nanostructured Li_2MnSiO_4/Al_2O_3 Supercapattery Electrode with Efficient Lithium-Ion Migratory Pathway. *Batter. Supercaps* **2018**, *1*, 223–235. [CrossRef]
36. Li, J.; Zhang, X.; Peng, R.; Huang, Y.; Guo, L.; Qi, Y. $LiMn_2O_4$/graphene composites as cathodes with enhanced electrochemical performance for lithium-ion capacitors. *RSC Adv.* **2016**, *6*, 54866–54873. [CrossRef]
37. Simon, P.; Burke, A. Nanostructured Carbons: Double-Layer Capacitance and More. *Electrochem. Soc. Interface* **2008**, *17*, 38–43. [CrossRef]

38. Amatucci, G.G.; Badway, F.; du Pasquier, A.; Amatucci, G.G.; Zheng, T.; Ohzuku, T.; Ueda, A.; Yamamoto, N. *The Nonaqueous Asymmetric Hybrid Technology: Materials, Electrochemical Properties and Performance in Plastic Cells*; Electrochemical Society: Pennington, NJ, USA, 2002; Volume MA.
39. Ohzuku, T.; Ueda, A.; Yamamoto, N. Zero-Strain Insertion Material of $Li[Li_{1/3}Ti_{5/3}]O_4$ for Rechargeable Lithium Cells. *J. Electrochem. Soc.* **1995**, *142*, 1431–1435. [CrossRef]
40. Chen, P.-C.; Shen, G.; Shi, Y.; Chen, H.; Zhou, C. Preparation and Characterization of Flexible Asymmetric Supercapacitors Based on Transition-Metal-Oxide Nanowire/Single-Walled Carbon Nanotube Hybrid Thin-Film Electrodes. *ACS Nano* **2010**, *4*, 4403–4411. [CrossRef]
41. Cottineau, T.; Toupin, M.; Delahaye, T.; Brousse, T.; Bélanger, D. Nanostructured transition metal oxides for aqueous hybrid electrochemical supercapacitors. *Appl. Phys. A* **2006**, *82*, 599–606. [CrossRef]
42. Sun, F.; Gao, J.; Zhu, Y.; Pi, X.; Wang, L.; Liu, X.; Qin, Y. A high performance lithium ion capacitor achieved by the integration of a Sn-C anode and a biomass-derived microporous activated carbon cathode. *Sci. Rep.* **2017**, *7*, 40990. [CrossRef]
43. Sui, Y.; Liu, C.; Zou, P.; Zhan, H.; Cui, Y.; Yang, C.; Cao, G. Polypyrrole Coated δ-MnO_2 Nanosheet Arrays as Highly Stable Lithium-Ion-Storage Anode Polypyrrole Coated δ-MnO_2 Nanosheet Arrays as Highly Stable Lithium-Ion-Storage Anode. *Dalton Trans.* **2020**, *49*, 7903–7913. [CrossRef]
44. Wang, X.; Liu, L.; Niu, Z. Carbon-based materials for lithium-ion capacitors. *Mater. Chem. Front.* **2019**, *3*, 1265–1279. [CrossRef]
45. Zhang, X.; Wang, L.; Liu, W.; Li, C.; Wang, K.; Ma, Y. Recent Advances in MXenes for Lithium-Ion Capacitors. *ACS Omega* **2020**, *5*, 75–82. [CrossRef] [PubMed]
46. Naskar, P.; Kundu, D.; Maiti, A.; Chakraborty, P.; Biswas, B.; Banerjee, A. Frontiers in Hybrid Ion Capacitors: A Review on Advanced Materials and Emerging Devices. *ChemElectroChem* **2021**, *8*, 1393–1429. [CrossRef]
47. Tušar, N.; Jank, S.; Gläser, R. Manganese-Containing Porous Silicates: Synthesis, Structural Properties and Catalytic Applications. *ChemCatChem* **2010**, *3*, 254–269. [CrossRef]
48. Li, H.; Zhang, W.; Sun, K.; Guo, J.; Yuan, K.; Fu, J.; Zhang, T.; Zhang, X.; Long, H.; Zhang, Z.; et al. Manganese-Based Materials for Rechargeable Batteries beyond Lithium-Ion. *Adv Energy Mater.* **2021**, *11*, 2100867. [CrossRef]
49. Zhang, W.; Zhai, X.; Zhang, Y.; Wei, H.; Ma, J.; Wang, J.; Liang, L.; Liu, Y.; Wang, G.; Ren, F.; et al. Application of Manganese-Based Materials in Aqueous Rechargeable Zinc-Ion Batteries. *Front. Energy Res.* **2020**, *8*, 195. [CrossRef]
50. Ma, S.-B.; Nam, K.-W.; Yoon, W.-S.; Yang, X.-Q.; Ahn, K.-Y.; Oh, K.-H.; Kim, K.-B. A novel concept of hybrid capacitor based on manganese oxide materials. *Electrochem. Commun.* **2007**, *9*, 2807–2811. [CrossRef]
51. Aravindan, V.; Gnanaraj, J.; Lee, Y.-S.; Madhavi, S. $LiMnPO_4$—A next generation cathode material for lithium-ion batteries. *J. Mater. Chem. A* **2013**, *1*, 3518–3539. [CrossRef]
52. Qin, Z.; Zhou, X.; Xia, Y.; Tang, C.; Liu, Z. Morphology controlled synthesis and modification of high-performance $LiMnPO_4$ cathode materials for Li-ion batteries. *J. Mater. Chem.* **2012**, *22*, 21144–21153. [CrossRef]
53. Yi, T.-F.; Mei, J.; Zhu, Y.-R. Key strategies for enhancing the cycling stability and rate capacity of $LiNi_{0.5}Mn_{1.5}O_4$ as high-voltage cathode materials for high power lithium-ion batteries. *J. Power Sources* **2016**, *316*, 85–105. [CrossRef]
54. Huang, Q.-Y.; Wu, Z.; Su, J.; Long, Y.-F.; Lv, X.-Y.; Wen, Y.-X. Synthesis and electrochemical performance of Ti–Fe co-doped $LiMnPO_4$/C as cathode material for lithium-ion batteries. *Ceram. Int.* **2016**, *42*, 11348–11354. [CrossRef]
55. Duan, J.; Hu, G.; Cao, Y.; Du, K.; Peng, Z. Synthesis of high-performance $LiMnPO_4$/C/rGO composite via a mechanical-activation-assisted polyol process. *Ionics* **2016**, *22*, 1541–1549. [CrossRef]
56. Dong, Y.; Zhao, Y.; Duan, H.; Liang, Z. Enhanced electrochemical performance of $LiMnPO_4$ by Li^+-conductive Li_3VO_4 surface coatings. *Electrochim. Acta* **2014**, *132*, 244–250. [CrossRef]
57. Moskon, J.; Pivko, M.; Jerman, I.; Tchernychova, E.; Logar, N.Z.; Zorko, M.; Selih, V.; Dominko, R.; Gaberscek, M. Cycling stability and degradation mechanism of $LiMnPO_4$ based electrodes. *J. Power Sources* **2016**, *303*, 97–108. [CrossRef]
58. Pitchai, R.; Thavasi, V.; Mhaisalkar, S.G.; Ramakrishna, S. Nanostructured cathode materials: A key for better performance in Li-ion batteries. *J. Mater. Chem.* **2011**, *21*, 11040–11051. [CrossRef]
59. Nolis, G.M.; Omenya, F.; Zhang, R.; Fang, B.; Upreti, S.; Chernova, N.A.; Wang, F.; Graetz, J.; Hu, Y.-Y.; Grey, C.P.; et al. Structure, defects and thermal stability of delithiated olivine phosphates. *J. Mater. Chem.* **2012**, *22*, 20482–20489. [CrossRef]
60. Herrera, J.O.; Camacho-Montes, H.; Fuentes, L.E.; Álvarez-Contreras, L. $LiMnPO_4$: Review on Synthesis and Electrochemical Properties. *J. Mater. Sci. Chem. Eng.* **2015**, *3*, 54–64. [CrossRef]
61. Xia, H.; Luo, Z.; Xie, J. Nanostructured $LiMn_2O_4$ and their composites as high-performance cathodes for lithium-ion batteries. *Prog. Nat. Sci. Mater. Int.* **2012**, *22*, 572–584. [CrossRef]
62. Chen, S.; Chen, Z.; Cao, C. Mesoporous Spinel LiMn2O4 Cathode Material by a Soft-templating Route. *Electrochim. Acta* **2016**, *199*, 51–58. [CrossRef]
63. Put, B.; Vereecken, P.M.; Labyedh, N.; Sepulveda, A.; Huyghebaert, C.; Radu, I.P.; Stesmans, A. High Cycling Stability and Extreme Rate Performance in Nanoscaled $LiMn_2O_4$ Thin Films. *ACS Appl. Mater. Interfaces* **2015**, *7*, 22413–22420. [CrossRef] [PubMed]
64. Hung, I.M.; Yang, Y.C.; Su, H.J.; Zhang, J. Influences of the Surfactant on the Performance of Nano-$LiMn_2O_4$ Cathode Material for Lithium-Ion Battery. *Ceram. Int.* **2015**, *41*, S779–S786. [CrossRef]
65. Plitz, I.; DuPasquier, A.; Badway, F.; Gural, J.; Pereira, N.; Gmitter, A.; Amatucci, G. The design of alternative nonaqueous high power chemistries. *Appl. Phys. A* **2006**, *82*, 615–626. [CrossRef]

66. Vijayan, S.; Kirubasankar, B.; Pazhamalai, P.; Solarajan, A.K.; Angaiah, S. Electrospun Nd^{3+}-Doped $LiMn_2O_4$ Nanofibers as High-Performance Cathode Material for Li-Ion Capacitors. *ChemElectroChem* **2017**, *4*, 2059–2067. [CrossRef]
67. Lu, J.; Chang, Y.-L.; Song, B.; Xia, H.; Yang, J.-R.; Lee, K.S.; Lu, L. High energy spinel-structured cathode stabilized by layered materials for advanced lithium-ion batteries. *J. Power Sources* **2014**, *271*, 604–613. [CrossRef]
68. West, N.; Ozoemena, K.I.; Ikpo, C.O.; Baker, P.G.; Iwuoha, E.I. Transition metal alloy-modulated lithium manganese oxide nanosystem for energy storage in lithium-ion battery cathodes. *Electrochim. Acta* **2013**, *101*, 86–92. [CrossRef]
69. Kim, D.K.; Muralidharan, P.; Lee, H.-W.; Ruffo, R.; Yang, Y.; Chan, C.K.; Peng, H.; Huggins, R.A.; Cui, Y. Spinel $LiMn_2O_4$ Nanorods as Lithium Ion Battery Cathodes. *Nano Lett.* **2008**, *8*, 3948–3952. [CrossRef]
70. Wang, F.; Xiao, S.; Zhu, Y.; Chang, Z.; Hu, C.; Wu, Y.; Holze, R. Spinel $LiMn_2O_4$ nanohybrid as high capacitance positive electrode material for supercapacitors. *J. Power Sources* **2014**, *246*, 19–23. [CrossRef]
71. Tianran, Z.; Daixin, L.; Tao, Z.; Jun, C. Understanding Electrode Materials of Rechargeable Lithium Batteries via DFT Calculations. *Prog. Nat. Sci. Mater. Int.* **2013**, *23*, 256–272.
72. Chen, Q.; Xiao, P.; Pei, Y.; Song, Y.; Xu, C.-Y.; Zhen, L.; Henkelman, G. Structural transformations in Li_2MnSiO_4: Evidence that a Li intercalation material can reversibly cycle through a disordered phase. *J. Mater. Chem. A* **2017**, *5*, 16722–16731. [CrossRef]
73. Wang, X.; Luo, S.; Li, P.; Zhan, Y.; Yan, S. Preparation and electrochemical performance of Li_2 $MnSiO_4$ cathode material doped with chromium on manganese site. *Int. J. Energy Res.* **2021**, *45*, 20483–20491. [CrossRef]
74. Hou, P.; Feng, J.; Wang, Y.; Wang, L.; Li, S.; Yang, L.; Luo, S.-H. Study on the properties of Li_2MnSiO_4 as cathode material for lithium-ion batteries by sol-gel method. *Ionics* **2020**, *26*, 1611–1616. [CrossRef]
75. Kumar, N.; Singh, M.; Kumar, A.; Tseng, T.-Y.; Sharma, Y. Facile and One-Step in Situ Synthesis of Pure Phase Mesoporous Li_2MnSiO_4/CNTs Nanocomposite for Hybrid Supercapacitors. *ACS Appl. Energy Mater.* **2020**, *3*, 2450–2464. [CrossRef]
76. Fisher, C.A.J.; Kuganathan, N.; Islam, M.S. Defect chemistry and lithium-ion migration in polymorphs of the cathode material Li_2MnSiO_4. *J. Mater. Chem. A* **2013**, *1*, 4207–4214. [CrossRef]
77. Wang, Y.; Wang, Y.; Jia, D.; Peng, Z.; Xia, Y.; Zheng, G. All-Nanowire Based Li-Ion Full Cells Using Homologous Mn_2O_3 and $LiMn_2O_4$. *Nano Lett.* **2014**, *14*, 1080–1084. [CrossRef]
78. Yang, X.; Qu, F.; Niu, H.; Wang, Q.; Yan, J.; Fan, Z. High-performance aqueous asymmetric supercapacitor based on spinel LiMn2O4 and nitrogen-doped graphene/porous carbon composite. *Electrochim. Acta* **2015**, *180*, 287–294. [CrossRef]
79. Lin, Y.-P.; Wu, N.-L. Characterization of $MnFe_2O_4/LiMn_2O_4$ aqueous asymmetric supercapacitor. *J. Power Sources* **2011**, *196*, 851–854. [CrossRef]
80. Pazhamalai, P.; Krishnamoorthy, K.; Sudhakaran, M.S.P.; Kim, S.J. Fabrication of High-Performance Aqueous Li-Ion Hybrid Capacitor with $LiMn_2$ O_4 and Graphene. *ChemElectroChem* **2016**, *4*, 396–403. [CrossRef]
81. Liu, L.; Diao, X.; He, Z.; Yi, Y.; Wang, T.; Wang, M.; Huang, J.; He, X.; Zhong, X.; Du, K. High-performance all-inorganic portable electrochromic Li-ion hybrid supercapacitors toward safe and smart energy storage. *Energy Storage Mater.* **2020**, *33*, 258–267. [CrossRef]
82. Prabaharan, S.; Star, R.A.; Kulkarni, A.R.; Michael, M. Nano-composite $LiMnPO_4$ as new insertion electrode for electrochemical supercapacitors. *Curr. Appl. Phys.* **2015**, *15*, 1624–1633. [CrossRef]
83. Xiang, J.; Zhang, P.; Lv, S.; Ma, Y.; Zhao, Q.; Sui, Y.; Ye, Y.; Qin, C. Spinel $LiMn_2O_4$ nanoparticles fabricated by the flexible soft template/Pichini method as cathode materials for aqueous lithium-ion capacitors with high energy and power density. *RSC Adv.* **2021**, *11*, 14891–14898. [CrossRef]
84. Chaturvedi, P.; Sil, A.; Sharma, Y. Energy storage performance of hybrid aqueous supercapacitor based on nano-Li_2MnSiO_4 and activated carbon. *Ionics* **2016**, *22*, 1719–1728. [CrossRef]
85. Chaturvedi, P.; Kumar, A.; Sil, A.; Sharma, Y. Cost effective urea combustion derived mesoporous-Li_2MnSiO_4 as a novel material for supercapacitors. *RSC Adv.* **2015**, *5*, 25156–25163. [CrossRef]
86. Zhang, Y.; Zhao, Y.; Deng, L. Enhanced electrochemical properties of $LiMnPO_4$/C via doping with Cu. *Ionics* **2012**, *18*, 573–578. [CrossRef]
87. Lee, E.-S.; Huq, A.; Chang, H.-Y.; Manthiram, A. High-Voltage, High-Energy Layered-Spinel Composite Cathodes with Superior Cycle Life for Lithium-Ion Batteries. *Chem. Mater.* **2012**, *24*, 600–612. [CrossRef]
88. Kang, B.J.; Joo, J.-B.; Lee, J.K.; Choi, W. Surface modification of cathodes with nanosized amorphous MnO_2 coating for high-power application in lithium-ion batteries. *J. Electroanal. Chem.* **2014**, *728*, 34–40. [CrossRef]
89. Bhatt, M.D.; O'Dwyer, C. Recent progress in theoretical and computational investigations of Li-ion battery materials and electrolytes. *Phys. Chem. Chem. Phys.* **2015**, *17*, 4799–4844. [CrossRef]
90. Julien, C.M.; Mauger, A.; Zaghib, K.; Groult, H. Comparative Issues of Cathode Materials for Li-Ion Batteries. *Inorganics* **2014**, *2*, 132–154. [CrossRef]
91. Liu, J.; Liu, X.; Huang, T.; Yu, A. Synthesis of nano-sized $LiMnPO_4$ and in situ carbon coating using a solvothermal method. *J. Power Sources* **2013**, *229*, 203–209. [CrossRef]
92. Liu, L.; Wang, T.; He, Z.; Yi, Y.; Wang, M.; Luo, Z.; Liu, Q.; Huang, J.; Zhong, X.; Du, K.; et al. All-solid-state electrochromic Li-ion hybrid supercapacitors for intelligent and wide-temperature energy storage. *Chem. Eng. J.* **2021**, *414*, 128892. [CrossRef]
93. Lu, J.; Zhan, C.; Wu, T.; Wen, J.; Lei, Y.; Kropf, A.J.; Wu, H.; Miller, D.J.; Elam, J.W.; Sun, Y.-K.; et al. Effectively suppressing dissolution of manganese from spinel lithium manganate via a nanoscale surface-doping approach. *Nat. Commun.* **2014**, *5*, 5693. [CrossRef] [PubMed]

94. Zhang, S.; Li, C.; Zhang, X.; Sun, X.; Wang, K.; Ma, Y. High Performance Lithium-Ion Hybrid Capacitors Employing Fe_3O_4–Graphene Composite Anode and Activated Carbon Cathode. *ACS Appl. Mater. Interfaces* **2017**, *9*, 17136–17144. [CrossRef] [PubMed]
95. Lu, C.; Wang, X.; Zhang, X.; Peng, H.; Zhang, Y.; Wang, G. Effect of graphene nanosheets on electrochemical performance of Li4Ti5O12 in lithium-ion capacitors. *Ceram. Int.* **2017**, *43*, 6554–6562. [CrossRef]
96. Xu, L.; Wang, S.; Zhang, X.; He, T.; Lu, F.; Li, H.; Ye, J. A facile method of preparing $LiMnPO_4$/reduced graphene oxide aerogel as cathodic material for aqueous lithium-ion hybrid supercapacitors. *Appl. Surf. Sci.* **2018**, *428*, 977–985. [CrossRef]
97. Chen, L.; Li, D.; Zheng, X.; Chen, L.; Zhang, Y.; Liang, Z.; Feng, J.; Si, P.; Lou, J.; Ci, L. Integrated nanocomposite of $LiMn_2O_4$/graphene/carbon nanotubes with pseudocapacitive properties as superior cathode for aqueous hybrid capacitors. *J. Electroanal. Chem.* **2019**, *842*, 74–81. [CrossRef]